International Journal of Fluid Power 8 (2007) No. 1 pp. 7-16

CASCADE CONTROL OF HYDRAULICALLY DRIVEN MANIPULATORS WITH FRICTION COMPENSATION

Antonio Carlos Valdiero[1], Raul Guenther[2], Edson Roberto De Pieri[3] and Victor Juliano De Negri[2]

[1] *Regional University of Northwestern Rio Grande do Sul State (UNIJUÍ), DETEC, Panambi, 98280-000 RS, Brazil*
[2] *Federal University of Santa Catarina (UFSC), EMC/CTC, Florianópolis, 88040-900 SC, Brazil*
[3] *Federal University of Santa Catarina (UFSC), DAS/CTC, Florianópolis, 88040-900 SC, Brazil*
valdiero@unijui.edu.br, guenther@emc.ufsc.br, edson@das.ufsc.br, victor@emc.ufsc.br

Abstract

This paper addresses the control of hydraulically driven manipulators with friction compensation. A cascade control strategy combined with a friction observer based on the Lugre friction model and including stiction effects is used and the convergence properties of the closed loop system are established using the Lyapunov method. This controller design and analysis are the new contributions of the paper. The theoretical analysis resulted in practical rules to tune the controller gains in order to guarantee its stability and the convergence of all the tracking errors, including the friction observer errors. An experimental implementation outlines the controller design details and illustrates the main features of the proposed strategy.

Keywords: hydraulically driven manipulators, cascade control, friction compensation, lyapunov based design

1 Introduction

Joint friction is one of the major limitations in performing high precision manipulation tasks. It affects both static and dynamic performance, and may cause instability when coupled to position or force control.

Friction compensation is particularly important for hydraulically driven manipulators in which, due to high supply pressure, tight sealing is required to prevent the actuators from significant internal leaks. This generates very high joint friction. Furthermore, nonlinear Stribeck friction, a well known source of stick-and-slip oscillations, has a particular importance in hydraulic systems. The aim of this paper is to establish the convergence properties of a hydraulically driven manipulator closed loop system with friction compensation based on the Lugre dynamic model (Canudas et al., 1995).

The controller is designed according to a cascade control strategy in which the hydraulically driven manipulator is interpreted as two interconnected subsystems: a mechanical subsystem driven by a hydraulic one as in Sepehri et al. (1990), Heintze et al. (1996), Guenther and De Pieri (1997), Lischinsky et al. (1999), Guenther et al. (2000), Honegger and Corke (2001), Sirouspour and Salcudean (2001), Cunha et al. (2002) and Valdiero (2005). The idea is to promote a fast loop in the hydraulic subsystem in order to generate forces in the hydraulic subsystem that allow the mechanical subsystem to track the desired trajectory.

This idea was formalized in Guenther and De Pieri (1997) and Guenther et al. (2000) taking into account the error during the hydraulic subsystem trajectory tracking and by presenting a stability proof of the whole interconnected system.

In Franco et al. (2004) the design and experimental implementation of controllers for hydraulic actuators is considered and two other controllers are proposed: a backstepping controller and a LQR-2DOF controller.

In Lischinsky et al. (1999) the authors outlined how to successfully use the friction compensation based on the Lugre model in a hydraulically driven manipulator by designing a cascade control with a sufficiently fast control loop in the hydraulic subsystem, without discussing the closed loop convergence properties.

In this paper we use the Lugre model, improved to include stiction effects as in Dupont et al. (2000). Additionally, we modify the friction observer used in Lischinsky et al. (1999) in order to establish closed loop convergence properties and rules for the controller gain tuning. We consider the manipulator dynamic passivity

This manuscript was received on 1 June 2006 and was accepted after revision for publication on 29 December 2006

properties, the nonlinear dynamics of the actuators, the strong coupling between the manipulator and the actuator dynamics and the nonlinear friction dynamics. The trajectory tracking closed loop convergence properties are established using the Lyapunov method and these theoretical results are experimentally validated using a hydraulically driven test manipulator.

In section 2, a dynamic model of the hydraulic robot is presented. The cascade controller is designed in section 3. Experimental results are shown and discussed in section 4. In section 5, the conclusions are presented.

2 Dynamic Model

In this section we present the system dynamics, including rigid manipulator dynamics, actuator dynamics and friction dynamics. Consider an *n* degrees of freedom (DOF) robot arm driven by *n* hydraulic cylinders as shown in Fig. 1. The generalized joint position vector is represented by *q* and the displacement vector of the hydraulic cylinders is *y*.

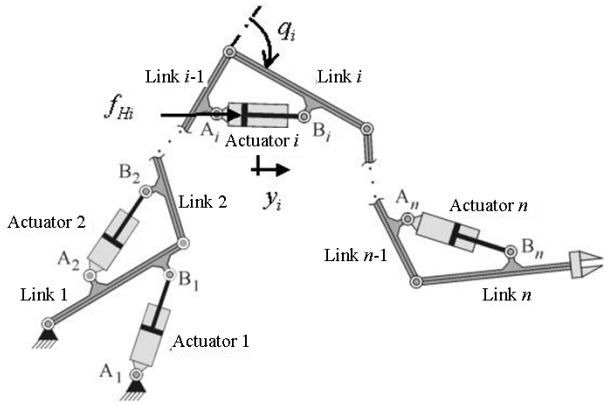

Fig. 1: *Robot arm driven by n hydraulic cylinders*

2.1 Rigid Robot Dynamics

The dynamic model of an *n*-link rigid robot may be described in the joint space as described in Sciavicco and Siciliano (2004):

$$H(q)\ddot{q} + C(q,\dot{q})\dot{q} + G(q) = \tau \tag{1}$$

where $H(q) \in \Re^{nxn}$ is the inertia matrix, $C(q,\dot{q}) \in \Re^{nxn}$ is the matrix containing centrifugal and Coriolis effects, $G(q) \in \Re^{n}$ is the vector representing gravitational effects, $q \in \Re^{n}$, $\dot{q} \in \Re^{n}$ and $\ddot{q} \in \Re^{n}$ are the joint position, velocity and acceleration vectors, respectively, and $\tau \in \Re^{n}$ is the joint torque vector. We consider that the joint friction can be neglected when compared to the actuator friction as given in Honegger and Corke (2001). This is valid for a roller bearing joint with low friction.

2.2 Hydraulic Actuator Dynamics

The joint torque vector is related to the actuator load force vector f_L by:

$$\tau = \bar{J}^T f_L \tag{2}$$

where $\bar{J}$ is a diagonal matrix that expresses the geometric relationship between the actuator motion and the corresponding joint motion (for details, see Valdiero (2005)).

Neglecting the actuator inertia and the gravitational forces that act on the pistons, the load force vector is

$$f_L = f_H - f_f \tag{3}$$

where f_H is the hydraulic force vector and f_f is the actuator friction force vector.

Substituting Eq. 2 and Eq. 3 into Eq. 1 results in

$$H(q)\ \ddot{q} + C(q,\dot{q})\ \dot{q} + \bar{J}^T f_f(q,\dot{q},z,\dot{z}) + G(q) = \bar{J}^T f_H \tag{4}$$

Considering a cylinder controlled by a critical centre four-way spool valve, the hydraulic force dynamics can be expressed in the following form:

$$\dot{f}_H = f_q(q,\dot{q}) + g_u(q, p_a, p_b, u) \tag{5}$$

where $u \in \Re^{n}$ is the control command vector, $f_q \in \Re^{n}$ is the vector of nonlinear functions that depends only on the motion variables and $g_u \in \Re^{n}$ is the vector of nonlinear functions that depends on the position vector *q*, on the cylinder chamber pressure vectors p_a and p_b, and on the control signal *u*. The detailed expressions of vectors f_q and g_u are given in Valdiero (2005).

The actuator friction forces vector f_f is obtained in the next section.

2.3 Actuator Friction Dynamics

We consider the actuator friction dynamics described by the Lugre model, proposed in Canudas et al. (1995) and improved by Dupont et al. (2000) in order to include stiction effects. This model is briefly presented in this section.

Using the Lugre model, the friction force vector in a hydraulic manipulator, considering the friction between the piston/cylinder surfaces, is represented by:

$$f_f = \Sigma_0 z + \Sigma_1 \dot{z} + \Sigma_2 \dot{y} \tag{6}$$

where $\Sigma_0 = diag[\sigma_{0i}]$ is the diagonal matrix whose elements represent the stiffness coefficient σ_{0i} of the microscopic deformation in actuator *i*; *z* is the average deflection vector of the asperities between surfaces (an internal state that can not be measured); $\Sigma_1 = diag[\sigma_{1i}]$ is the diagonal matrix whose elements represent the damping coefficient σ_{1i} associated with dz_i/dt in actuator *i*; $\Sigma_2 = diag[\sigma_{2i}]$ is the diagonal matrix whose elements represent the viscous friction coefficient σ_{2i} in actuator *i*; $\dot{y}$ is the actuator velocity vector.

The average deflection dynamics are given in Dupont et al. (2000):

$$\dot{z} = \dot{y} - A(z,\dot{y})z \tag{7}$$

where $A(z,\dot{y})$ is the diagonal matrix defined in Eq. 8:

$$A(z,\dot{y}) = diag\left[\alpha_i(z_i,\dot{y}_i)\frac{\sigma_{0i}}{g_{ss\,i}(\dot{y}_i)}sign(\dot{y}_i)\dot{y}_i\right] \geq 0 \qquad (8)$$

where $\alpha_i(z_i,\dot{y}_i)$ is a function used to represent the stiction and $g_{ss\,i}(\dot{y})$ is a function that describes the steady state friction characteristics.

It is well known that the friction force in the seal of a piston is highly influenced by the hydraulic pressure. In the model presented above this influence can be included by considering that the stiffness coefficients σ_{0i} and damping coefficients σ_{1i} depend on the hydraulic pressure.

In this paper the hydraulic pressure influence on the friction force is not taken into account since both coefficients are considered to be constant. The consequences of this assumption will be discussed in section 3.4.

2.4 System Dynamics

The entire system dynamics is given by Eq. 4, 5 and 7.

3 The Cascade Control Strategy

In hydraulically driven manipulators the trajectory tracking problem consist of the design of a control law for the control vector u such that the vector $[q(t) \quad \dot{q}(t)]^T$ tracks a desired trajectory vector $[q_d(t) \quad \dot{q}_d(t)]^T$, where $q_d(t)$ is the desired joint position vector. To achieve this end we define the error in the applied hydraulic forces as:

$$\tilde{f}_H = f_H - f_{Hd} \qquad (9)$$

where f_{Hd} is the desired hydraulic force vector designed so as to obtain the trajectory tracking. Substituting Eq. 9 into Eq. 4 gives:

$$H(q)\ \ddot{q} + C(q,\dot{q})\ \dot{q} + \bar{J}^T f_f(q,\dot{q},z,\dot{z}) + G(q) = \bar{J}^T f_{Hd} + \bar{J}^T \tilde{f}_H \qquad (10)$$

Including Eq. 7 and 5 reproduced below

$$\dot{z} = \dot{y} - A(z,\dot{y})z$$

$$\dot{f}_H = f_q(q,\dot{q}) + g_u(q,p_a,p_b,u)$$

The system described by Eq. 10, 7 and 5 is in the cascade form. Equations 10 and 7 represent the mechanical subsystem with friction, driven by a desired hydraulic force vector f_{Hd} and subjected to an input disturbance $\tilde{f}_H$. Equation 5 represents the hydraulic subsystem.

The design of the cascade controller for the system described above can be summarized as:

- Compute a control law f_{Hd} for the mechanical subsystem in Eq. 10 such that the joint position vector $q(t)$ achieves a desired trajectory $q_d(t)$ taking into account the presence of the disturbance $\tilde{f}_H$;
- Compute a control law u for the hydraulic subsystem in Eq. 5 such that f_H tracks the desired hydraulic force vector f_{Hd} as close as possible.

In this paper the design of the mechanical subsystem control law f_{Hd} is based on the controller proposed by Slotine and Li (1988) which includes a friction compensation scheme. The friction compensation is based on an observer, designed using the Lugre friction model. The control law u is synthesized to achieve good tracking performance characteristics related to the hydraulic subsystem. A cascade control structure block diagram is shown in Fig. 2. The friction force observer and the controllers are then described.

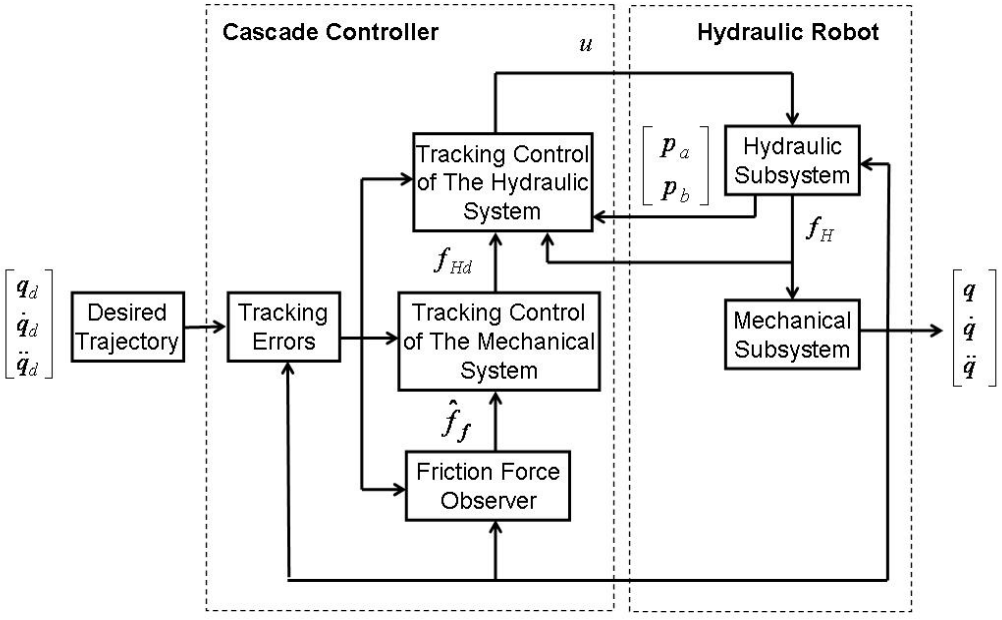

Fig. 2: *Cascade control structure block diagram*

3.1 The Friction Force Observer

According to Canudas et al. (1995) the estimated friction force vector $\hat{f}_f(q,\dot{q},\hat{z},\dot{\hat{z}})$ is given by:

$$\hat{f}_f = \Sigma_0\hat{z} + \Sigma_1\dot{\hat{z}} + \Sigma_2\dot{y} \tag{11}$$

where $\hat{z}$ is the estimated friction internal state vector. In this paper we propose that it is given by:

$$\dot{\hat{z}} = \dot{y} - \hat{A}(\hat{z},\dot{y})\hat{z} - K_{obs}\overline{J}s_0 \tag{12}$$

where $K_{obs} > 0$ is the observer gain diagonal matrix; s_0 is the measure of the velocity tracking error defined in Eq. 21; $\hat{A}(\hat{z},\dot{y})$ is the diagonal matrix defined in Eq. 13:

$$\hat{A}(\hat{z},\dot{y}) = diag\left[\hat{\alpha}_i(\hat{z}_i,\dot{y}_i)\frac{\sigma_{0i}}{g_{ss\,i}(\dot{y}_i)}m(\dot{y}_i)\dot{y}_i\right] \geq 0 \tag{13}$$

where $\hat{\alpha}_i(\hat{z}_i,\dot{y}_i)$ is the function used to represent the stiction as $\alpha_i(z_i,\dot{y}_i)$ in Eq. 8, calculated using the estimated friction state $\hat{z}_i$. The function $m(\dot{y}_i)$ is introduced to smoothen the signal function $sign(\dot{y}_i)$ in order to calculate the desired hydraulic force time derivative $\dot{f}_{Hd}$, employed to obtain the trajectory tracking in the hydraulic subsystem (see Eq. 18) based on Eq. 14.

3.2 The Tracking Control of the Mechanical Subsystem

Based on Slotine and Li (1988) and including the friction compensation, we propose the following control law to obtain trajectory tracking in the mechanical subsystem:

$$\begin{aligned} f_{Hd} = (\overline{J}^T)^{-1}[H(q)\ddot{q}_r + C(q,\dot{q})\dot{q}_r + G(q) \\ -K_{P1}\tilde{q} - K_D s_0] + \hat{f}_f(q,\dot{q},\hat{z},\dot{\hat{z}}) \end{aligned} \tag{14}$$

where K_{P1} and K_D are diagonal positive definite matrices; $\tilde{q}$ is the tracking joint error vector defined in Eq. 15; $\dot{q}_r$ is the joint reference velocity vector defined in Eq. 16; s_0 is a measure of the velocity tracking error vector Eq. 17; $\hat{f}_f(q,\dot{q},\hat{z},\dot{\hat{z}})$ is the estimated friction forces vector calculated in Eq. 11.

$$\tilde{q} = q - q_d \tag{15}$$

$$\dot{q}_r = \dot{q}_d - \Lambda\tilde{q} \tag{16}$$

$$s_0 = \dot{q} - \dot{q}_r = \dot{\tilde{q}} + \Lambda\tilde{q} \tag{17}$$

where Λ is a diagonal positive definite matrix.

3.3 Tracking Control of the Hydraulic Subsystem

In order to obtain the force tracking in the hydraulic subsystem we propose the following control law:

$$g_u(q, p_a, p_b, u) = -f_q(q,\dot{q}) + \dot{f}_{Hd} - K_P\tilde{f}_H - \overline{J}s_0 \tag{18}$$

where K_P is a positive definite gain diagonal matrix. Note that the control vector u is obtained using g_u given by Eq. 18.

3.4 The Cascade Controller Stability

The cascade controller stability is presented in detail in appendix. In this section we present a qualitative discussion in order to outline the closed loop convergence properties, and the gain tuning.

Theoretically we established that the controller gains can be chosen in order to obtain the convergence of the tracking errors, $\tilde{q}(t)$ and $\dot{\tilde{q}}(t)$, to a residual set R as $t \to \infty$. Moreover, the set R depends on the friction characteristics and on the controller gains.

To this end the friction force observer gains should be designed in order to satisfy the equation below:

$$K_{obs\,i} < 2\sigma_{0i}/(\sigma_{1i}\left|\overline{J}_i\right|) \tag{19}$$

where σ_{0i} is the stiffness coefficient of the microscopic deformation in actuator i, σ_{1i} is the damping coefficient associated with dz_i/dt in actuator i, and $\left|\overline{J}_i\right|$ is the norm of the i-th element of the $\overline{J}$ diagonal matrix which expresses the geometric relationship between the actuator motion and the corresponding joint motion.

To obtain the convergence of the tracking errors, besides condition 19, the mechanical subsystem gains given in matrix K_D have to satisfy the following condition:

$$K_{Di} > 1/2\ \left[\left|\overline{J}_i\right|\hat{A}_{imax} - \overline{J}_i^2 K_{obs\,i}\right]\sigma_{1i} \tag{20}$$

where $\hat{A}_{i\,max} = \hat{A}_i(\hat{z}_i, \dot{y}_{imax})$ is an upper limit for the i-th diagonal element of the matrix defined in Eq. 13, calculated according the upper limit to the i-th actuator velocity, $\dot{y}_{i\,max}$, given by an initial condition.

Under conditions 19 and 20 the error state vector defined as $\rho = [s_0^T \quad \tilde{q}^T \quad \tilde{z}^T \quad \tilde{f}_H^T]^T$ tends to a residual set given by:

$$\|\rho\| > \overline{D}/\alpha \tag{21}$$

where $\overline{D}$ is an upper limit to the so called "disturbance vector" $D(\rho)$, which depends on the friction characteristics and on the smoothing function $m(\dot{y}_i)$ (see the appendix), and α is a positive constant which is dependent on the controller gains (see Eq. A23 in appendix).

Remark: Since the stiffness coefficients σ_{0i} and the damping coefficients σ_{1i} may be dependent on the hydraulic pressure, condition 19 should be satisfied considering the case in which the relation between the coefficients is minimal. Furthermore, condition 20 should be satisfied considering the maximum value of the damping coefficient σ_{1i}.

With the equipment friction parameters determined taking the above remark into account and choosing a smoothing function, the residual set $\|\rho\|$ given in Eq. 21 is dependent on the mechanical subsystem controller gains given in matrices Λ, K_{P1} and K_D, on the hydraulic subsystem gains (matrix K_P) and on the friction force observer gains (matrix K_{obs}). The design of these gains is presented in detail in Cunha et al. (2002).

The experimental results presented in section 4 illustrate these results.

4 Experimental Results

The cascade control strategy was implemented on the 2 DOF hydraulically driven test manipulator shown in Fig. 3, installed at LASHIP (in the Federal University of Santa Catarina).

This manipulator is composed of the main components shown in Table 1, a data acquisition and control board DS 1104 dSPACE and a conditioning and power hydraulic unit. The experimental setup is described in detail in Valdiero (2005).

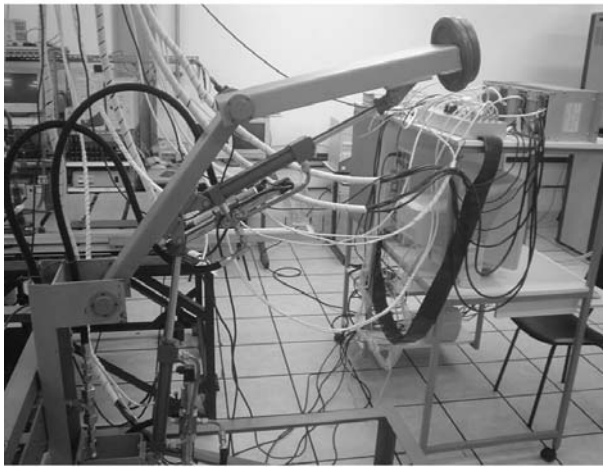

Fig. 3: *Experimental Hydraulic Robot Arm*

Table 1: Main components from experimental test apparatus on joint 1

Component	Make	Catalog code
Hydraulic cylinder	BOSCH REXROTH	CDT3MP5/25/18/200/ Z1X/B1CHDTWW
Proportional valve	BOSCH REXROTH	4WRE6E1-08-2X/G24K4/V
Pressure sensors	ZÜRICH	PSI-420 (0-100 bar)
Incremental Encoder	HOHNER	7510-0622-0500

The proportional valve has a dead zone whose parameters were identified observing the dynamic behavior of the pressure in the valve gaps (Valdiero, 2005). The harmful effects of the dead zone are compensated using an inverse as in Cunha et al. (2002).

The tests were performed using a polynomial desired trajectory on joint 1, with joint 2 stopped at its maximum position. The desired trajectory of joint 1 is shown in Fig. 4 and can be described by Eq. 22.

$$q_{d1}(t)=\begin{cases}0.43+(-0.02t^7+0.4t^6-2.8t^5+7t^4)10^{-3} & for\ \ t<6\\ 0.69 & for\ \ 6\le t\le 12\\ 0.69-(-0.02t^7+0.4t^6-2.8t^5+7t^4)10^{-3} & for\ \ 12<t<18\\ 0.43 & for\ \ t>18\end{cases} \quad (22)$$

The position and velocity reference trajectories of actuator 1 corresponding to the joint 1 position reference given in Eq. 22 are shown in Fig. 5 and Fig. 6, respectively.

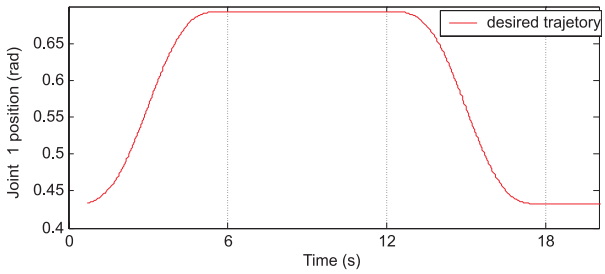

Fig. 4: *Joint 1 position reference.*

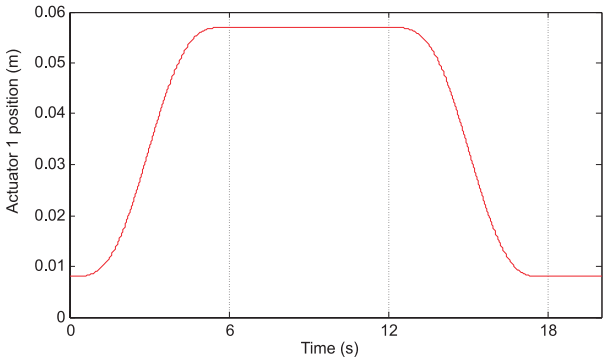

Fig. 5: *Actuator 1 position reference.*

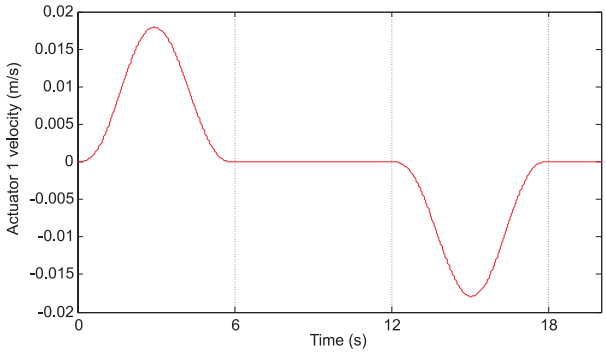

Fig. 6: *Actuator 1 velocity reference.*

The cascade controller is given by the friction force observer (Eq. 11), the mechanical subsystem control law (Eq. 18), and by the solution of Eq. 25.

To calculate the estimated friction force we need to obtain the function $g_{ss1}(\dot{y})$, the viscous friction coefficient σ_{21}, and the dynamic parameters σ_{01} and σ_{11} in actuator 1.

The function $g_{ss1}(\dot{y})$ and the viscous friction coefficient σ_{21} are obtained experimentally using the static friction map (Fig. 7), in which the friction forces corresponding to steady state velocities are plotted.

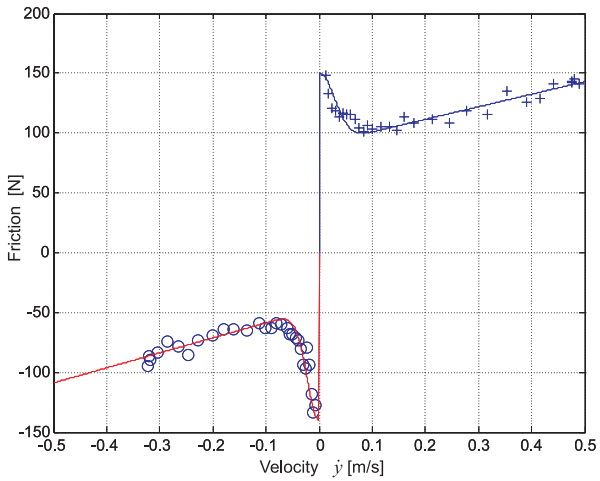

Fig. 7: *Static friction map for actuator 1 with experimental values and fitting curves*

Figure 7 shows the adjusted functions $g_{ss1}(\dot{y})$ and the viscous friction. The corresponding viscous coefficients are σ_{21}= 105.15 Ns/m for $\dot{y} > 0$ and σ_{21}= 125.41 Ns/m for $\dot{y} < 0$.

According to Canudas and Lischinsky (1997), the dynamic parameters σ_{01} and σ_{11} are calculated using an experimental procedure combined with a numerical non-linear optimization. For hydraulic actuators this experimental procedure is difficult to use because it is based on detecting stick-slip movements and velocity inversions. These inversions are difficult to detect due to valve internal leakages and a residual dead zone. Similar difficulties are observed in pneumatic actuators (Perondi, 2002).

For pneumatic actuators, Perondi (2002) compares experimental results, obtained according to Canudas and Lischinsky (1997), with parameters adjusted by simulations, and concludes that the dynamic parameter values obtained by simulations are lower than measured values.

In this paper, the dynamic parameters σ_{01} and σ_{11} were adjusted by simulation in order to obtain acceptable microscopic deformations considering the sample rate time limitations to implement the friction observer in real time.

According to Armstrong and Canudas (1996), the microscopic deformations in the pre-sliding phase are in the 1 to 50 μm range. This allows us to estimate that σ_{01}= 0.5 x 10^6 N/m for both situations ($\dot{y} > 0$ and $\dot{y} < 0$). Considering that the dynamic parameter σ_{11} has to introduce an adequate damping into the friction model in the pre-sliding movement phase and has to be adjusted in order to assure the passivity propriety according the condition introduced in (Barahanov and Ortega, 2000), we estimate σ_{11}= 127.2 Ns/m for $\dot{y} > 0$ and σ_{11} = 49.6 Ns/m for $\dot{y} < 0$.

The friction observer gain is chosen according to condition 19 and tuned in order to obtain a smooth response. In this way we obtain K_{obs} = 0.01.

The gain K_D is chosen to satisfy condition 20 and is tuned together with the other control gains in order to obtain a response without arm vibrations and a sufficiently smooth control signal (see details in Cunha et al. 2002. The resulting control gains for actuator 1 are λ = 40, K_P = 300, K_D = 300, K_{P1} = 20.

The estimated friction force during the movement described in Figs. 5 and 6 is shown in Fig. 8.

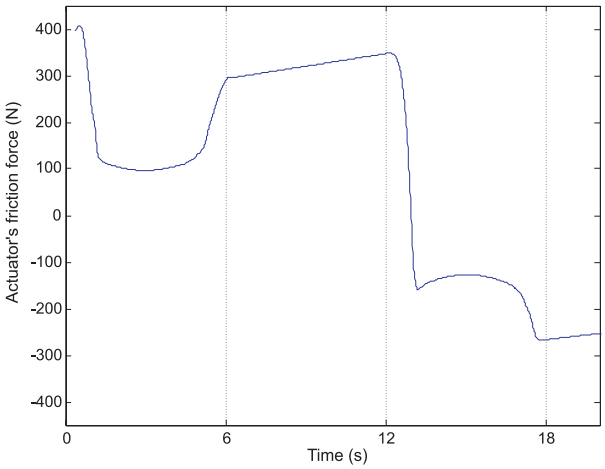

Fig. 8: *Estimated Friction Force (Actuator 1).*

Note that the estimated friction force increases in the static friction range (between 6 and 12 seconds) due to the integral action on the friction observer. Due to this, the friction observer tends to compensate the closed loop system parametric uncertainties by overestimating the static friction force.

Figure 9 shows the position tracking results obtained in the first joint of the manipulator, with and without the proposed friction compensation. The tracking errors converge to residual sets in both cases and in the case including friction compensation the residual set is smaller than in the case without friction compensation.

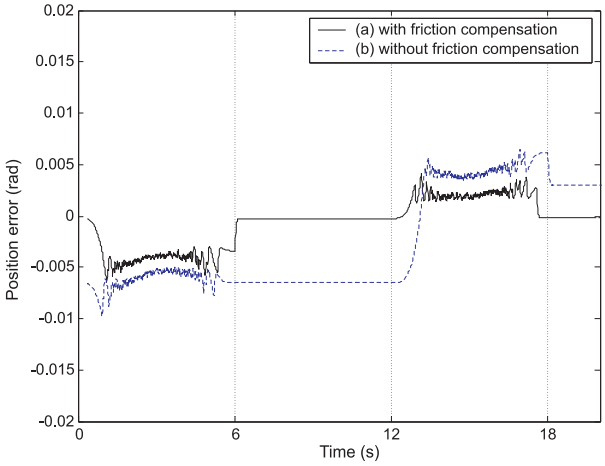

Fig. 9: *Tracking Error: (a) with and (b) without Friction Compensation (Joint 1).*

5 Conclusions

In this paper a cascade control with friction compensation for hydraulically driven manipulators was presented. The controller considers the full dynamic model of hydraulically driven manipulators and the friction forces in the actuators. These friction forces are compensated using an observer based on the Lugre friction model. The Lyapunov stability method is used to establish the convergence of the closed loop tracking errors to a residual set in a local sense. This theoretical analysis highlights that the residual set depends on the friction characteristics and on the controller design. Furthermore, the analysis results in design rules for the controller gain tuning. These results were confirmed experimentally.

Nomenclature

f_f	actuator friction force	[N]
f_H	hydraulic force	[N]
f_{Hd}	desired hydraulic force	[N]
f_L	actuator load force	[N]
p_a	pressure in cylinder chamber 1	[N/m²]
p_b	pressure in cylinder chamber 2	[N/m²]
q	joint position	[rad]
q_d	desired trajectory	[rad]
u	voltage applied to the servo valve	[V]
z	average deflection	[m]
y	actuator piston position	[m]
σ_0	stiffness coefficient	[N/m]
σ_1	damping coefficient	[Ns/m]
σ_2	viscous friction coefficient	[Ns/m]
τ	joint torque	[Nm^2]

Acknowledgments

This work was partially supported by "Conselho Nacional de Desenvolvimento Científico e Tecnológico (CNPq)", Brasil.

References

Armstrong, B. and **Canudas-De-Wit, C.** 1996. Friction modeling and compensation. *The control handbook*. CRC Press, 1996. pp. 1369-1382.

Barahanov, N. and **Ortega R.** 2000. Necessary and sufficient conditions for passivity of the LuGre friction model. *IEEE Transactions on Automatic Control*. Vol.45, No.4, pp. 830-832.

Canudas-De-Wit, C., **Olsson, H.**, **Aström, K. J.** and **Lischinsky, P.** 1995. A new model for the control of systems with friction. *IEEE Transactions on Automatic Control*, Vol. 40, No. 3, pp. 419-425.

Canudas-De-Wit, C. and **Lischinsky, P.** 1997. Adaptive friction compensation with partially known dynamic friction model. *International Journal of Adaptive Control and Signal Processing*, Vol. 11, pp.65-80.

Cunha, M. A. B., **Guenther, R.**, **De Pieri, E. R.** and **De Negri, V. J.** 2002. Design of cascade controllers for a hydraulic actuator. *International Journal of Fluid Power*, Vol. 3, No. 2, pp. 35-46.

Dupont, P., **Armstrong, B.** and **Hayward, V.** 2000. Elasto-plastic friction model: contact compliance and stiction. *Proceedings of the American Control Conference*, pp. 1072-1077.

Franco, A. L. D., **De Pieri, E. R.**, **Castelan, E. B.**, **Guenther, R.** and **Valdiero, A. C.** 2004. Design and experimental evaluation of position controllers for hydraulic actuators: backstepping and LQR-2DOF controllers. *International Journal of Fluid Power*, Vol. 5, No. 3, pp. 39-48.

Guenther, R. and **De Pieri, E. R.** 1997. Cascade control of the hydraulic actuators. *Journal of the Brazilian Society Mechanical Sciences*, Vol. 19, No. 2, pp. 108-120.

Guenther, R., **Cunha, M. A. B.**, **De Pieri, E. R.** and **De Negri, V. J.** 2000. VS-ACC Applied to a Hydraulic Actuator. *Proceedings of American Control Conference*, pp. 4124-4128.

Heintze, J., **Teerhuis, P. C.** and **Van-Der-Weiden, A. J. J.** 1996. Controlled hydraulics for a direct drive brick laying robot. *Automation in Construction*, pp. 23-29.

Honegger, M. and **Corke, P.** 2001. Model-based control of hydraulically actuated manipulators. *Proceedings of IEEE International Conference on Robotics and Automation*, Vol. 3, pp. 2553 –2559.

Lischinsky, P., **Canudas-de-Wit, C.** and **Morel, G.** 1999. Friction Compensation for an Industrial Hydraulic Robot. *IEEE Control Systems Magazine*, Vol. 19, pp. 25-32.

Perondi, E. A. 2002. *Cascade Nolinear Control with Friction Compensation of a Pneumatic Servo Positioning* (In Portuguese). PhD thesis. Mechanical Engineering Department, Federal University of Santa Catarina, Brazil.

Ramirez, A. R. G. 2003. *Position control of robotic manipulators with flexible transmissions considering the friction compensation.* (In Portuguese), PhD Thesis, Mechanical Engineering Department, Federal University of Santa Catarina, Brazil.

Sciavicco, L. and **Siciliano, B.** 2004. *Modeling and control of robot manipulators.* Springer Verlag.

Sepehri, N., **Dumont, G. A. M.**, **Lawrence, P. D.** and **Sassani, F.** 1990. Cascade control of hydraulically actuated manipulators. *Robotica*, Vol. 8, pp. 207-216.

Sirouspour, M. R. and **Salcudean, S. E.** 2001. Nonlinear control of a hydraulic parallel manipulator. *Proceedings of the IEEE International Conference on Robotics and Automation*, Vol. 4, pp. 3760-3765.

Slotine, J.-J. E. and **Li, W.** 1988. Adaptive manipulator control: a case study. *IEEE Transaction on Automatic Control*, pp. 33-44.

Slotine, J.-J. E. and **Li, W.** 1991. *Applied nonlinear control.* Prentice Hall.

Valdiero, A. C. 2005. *Control of Hydraulic Robots with Friction Compensation* (In Portuguese). PhD thesis. Mechanical Engineering Department, Federal University of Santa Catarina, Brazil.

Appendix

In this appendix the cascade controller stability analysis is presented in more details.

To this end some aspects of the friction force observer, of the tracking control of the mechanical subsystem and of the tracking control of the hydraulic subsystem should be pointed out.

Friction force observer: the smoothing function used in Eq. 12 is given by:

$$m(\dot{y}_i) = 2/\pi \arctan(k_v \dot{y}_i) \geq 0 \tag{A1}$$

where k_v is a positive constant.

By using the estimated matrix defined in Eq. 13 in the friction observer an error given by the matrix $\tilde{A}(z,\hat{z},\dot{y}) = A(z,\dot{y}) - \hat{A}(\hat{z},\dot{y})$ is introduced. Calculating this error matrix using Eq. 8 and Eq. 13 results in:

$$\begin{aligned}\tilde{A}(z,\hat{z},\dot{y}) = diag[&(\alpha_i(z_i,\dot{y}_i)sign(\dot{y}_i) \\ &-\hat{\alpha}_i(\hat{z}_i,\dot{y}_i)m(\dot{y}_i))\frac{\sigma_{0i}\dot{y}_i}{g_{ssi}(\dot{y}_i)}]\end{aligned} \tag{A2}$$

The elements of this matrix are limited, since the functions $\alpha_i(z_i,\dot{y}_i)$ and $\hat{\alpha}_i(\hat{z}_i,\dot{y}_i)$ are nonnegative and limited (see Dupont et al. (2000)), and the function $g_{ssi}(\dot{y})$ is limited by the Coulomb friction force and the static friction force.

Defining the error in the estimated friction state vector as $\tilde{z}(=z-\hat{z})$, the dynamics of this error are obtained using Eq. 12, 7 and A2, and are calculated by:

$$\dot{\tilde{z}} = -\tilde{A}(z,\hat{z},\dot{y})z - \hat{A}(\hat{z},\dot{y})\tilde{z} + K_{obs}\bar{J}s_0 \tag{A3}$$

Using Eqs. 6 and 11, the estimated friction force error $\tilde{f}_f = f_f - \hat{f}_f$ is written as:

$$\tilde{f}_f = \Sigma_0\tilde{z} + \Sigma_1\dot{\tilde{z}} \tag{A4}$$

Mechanical subsystem: In this subsystem the error dynamics is obtained applying the control law (Eq. 14) to the mechanical subsystem with friction (Eq. 10) using Eq. A3, A4 and the error definitions given by Eq. 15, 16 and 17. So, we arrive at:

$$\begin{aligned}&H(q)\dot{s}_0 + [C(q,\dot{q}) + K_D]s_0 + K_{P1}\tilde{q} \\ &+\bar{J}^T\Sigma_0\tilde{z} + \bar{J}^T\Sigma_1\dot{\tilde{z}} = \bar{J}^T\tilde{f}_H\end{aligned} \tag{A5}$$

To perform the Lyapunov stability analysis presented in the sequence consider the nonnegative function:

$$\begin{aligned}V_1(s_0,\tilde{q},\tilde{z}) = &\frac{1}{2}s_0^T H(q)s_0 + \frac{1}{2}\tilde{q}^T K_{P1}\tilde{q} \\ &+\frac{1}{2}\tilde{z}^T\Sigma_0 K_{obs}^{-1}\tilde{z}\end{aligned} \tag{A6}$$

Using Eq. A5, the time derivative of Eq. A6 along the mechanical subsystem trajectories is given by:

$$\begin{aligned}\dot{V}_1(s_0,\tilde{q},\tilde{z}) = &-s_0^T[K_D + \bar{J}^T\Sigma_1 K_{obs}\bar{J}]s_0 \\ &-\tilde{q}^T K_{P1}\Lambda\tilde{q} - \tilde{z}^T\Sigma_0 K_{obs}^{-1}\hat{A}(\hat{z},\dot{y})\tilde{z} + s_0^T\bar{J}^T\tilde{f}_H \\ &+s_0^T\bar{J}^T\Sigma_1\hat{A}(\hat{z},\dot{y})\tilde{z} + s_0^T\bar{J}^T\Sigma_1\tilde{A}(z,\hat{z},\dot{y})z \\ &-\tilde{z}^T\Sigma_0 K_{obs}^{-1}\tilde{A}(z,\hat{z},\dot{y})z\end{aligned} \tag{A7}$$

where the screw symmetry property of the robot dynamics (Sciavicco and Siciliano, 2004) was employed.

Hydraulic subsystem: in this subsystem, the error in the hydraulic force tracking dynamics is obtained by combining Eq. 5, 18 and 9, and results:

$$\dot{\tilde{f}}_H = -K_P\tilde{f}_H - \bar{J}s_0 \tag{A8}$$

The design of the gain matrix K_P is based on the nonnegative function V_2 defined as:

$$V_2 = 1/2\,\tilde{f}_H{}^T\tilde{f}_H \tag{A9}$$

The time derivative of the function V_2 along the error system trajectories (Eq. A8) is given by:

$$\dot{V}_2 = -\tilde{f}_H{}^T K_P\tilde{f}_H - \tilde{f}_H{}^T\bar{J}s_o \tag{A10}$$

The stability analysis is performed considering the cascade controlled hydraulically driven manipulator system with the friction observer. The resulting closed loop system is Ω = {(10), (7), (5), (11), (14), (18)}.

We assume that the desired joint position vector $q_d(t)$ and its derivatives up to third order are uniformly bounded.

Tracking error convergence properties: When all the system parameters are known, given an initial condition, the controller gains can be chosen in order to obtain the convergence of the tracking errors, $\tilde{q}(t)$ and $\dot{\tilde{q}}(t)$, to a residual set *R* as $t \to \infty$. The set *R* depends on the friction characteristics and on the controller gains.

Proof: Consider the lower bound function obtained using Eq. A6 and Eq. A9:

$$V(s_0,\tilde{q},\tilde{z},\tilde{f}_H) = V_1(s_0,\tilde{q},\tilde{z}) + V_2 \tag{A11}$$

In a matrix equation form this expression results in:

$$V = 1/2\,\rho^T N_1\rho \tag{A12}$$

where the error state vector is defined as $\rho = [s_0{}^T \quad \tilde{q}^T \quad \tilde{z}^T \quad \tilde{f}_H{}^T]^T$ and the matrix N_1 is

$$N_1 = \begin{bmatrix} H & 0 & 0 & 0 \\ 0 & K_{P1} & 0 & 0 \\ 0 & 0 & \Sigma_0 K_{obs}^{-1} & 0 \\ 0 & 0 & 0 & 1 \end{bmatrix} \quad \text{(A13)}$$

The time derivative of Eq. A11 along the systems trajectories is obtained using Eq. A7 and A10:

$$\dot{V} = -\rho^T N_2 \rho + \rho^T D \quad \text{(A14)}$$

where the matrix N_2 and the "disturbance vector" D are given by:

$$N_2 = \begin{bmatrix} K_D + \bar{J}^T \Sigma_1 K_{obs} \bar{J} & 0 & 1/2 \ \bar{J}^T \Sigma_1 \hat{A}(\hat{z}, \dot{y}) & 0 \\ 0 & K_{P1} \Lambda & 0 & 0 \\ 1/2 \ \bar{J}^T \Sigma_1 \hat{A}(\hat{z}, \dot{y}) & 0 & \Sigma_0 K_{obs}^{-1} \hat{A}(\hat{z}, \dot{y}) & 0 \\ 0 & 0 & 0 & K_P \end{bmatrix} \quad \text{(A15)}$$

$$D = \begin{bmatrix} (\bar{J}^T \Sigma_1 \tilde{A}(z, \hat{z}, \dot{y}) z)^T \\ 0^T \\ (-\Sigma_0 K_{obs}^{-1} \tilde{A}(z, \hat{z}, \dot{y}) z)^T \\ 0^T \end{bmatrix} \quad \text{(A16)}$$

The matrix N_2 is state dependent because the matrices $\bar{J}$ and $\hat{A}(\hat{z}, \dot{y})$ are state dependent. In the sequence we establish the conditions to make this matrix be uniformly positive definite.

First we observe that the matrices Σ_1 and K_{obs} are diagonal positive definite (see Eq. 6 and Eq. 12). This implies that $K_D + \bar{J}^T \Sigma_1 K_{obs} \bar{J} > 0$.

The diagonal matrix $\hat{A}(\hat{z}, \dot{y})$, defined in Eq. 13, is null in the static friction range ($\dot{y} = 0$) and is positive definite out of this range ($\dot{y} \neq 0$).

Out of the static friction range ($\dot{y} \neq 0$), using the Gershgorin theorem it should be observed that the matrix N_2 in Eq. A15 is positive definite if:

$$\left| \sigma_{0i} K_{obs\,i}^{-1} \hat{A}_i(\hat{z}_i, \dot{y}_i) \right| > \left| 1/2 \bar{J}_i \sigma_{1i} \hat{A}_i(\hat{z}_i, \dot{y}_i) \right| \quad \text{(A17)}$$

for i=1, n where σ_{0i}, $K_{obs\,i}$, $\bar{J}_i$, $\hat{A}_i(\hat{z}_i, \dot{y}_i)$ and σ_{1i} are the elements of the diagonal matrices Σ_0, K_{obs}, $\bar{J}$, $\hat{A}(\hat{z}, \dot{y})$ and Σ_1, respectively. Considering the elements signal results in:

$$K_{obs\,i} < 2\sigma_{0i} / (\sigma_{1i} \left| \bar{J}_i \right|) \quad \text{(A18)}$$

The matrix $\bar{J}$ elements are limited (Valdiero, 2005), i.e. $\left| \bar{J}_i \right|$ is limited, and the gain $K_{obs\,i}$ should be chosen in order to satisfy the condition expressed in Eq. A17.

$$\left| K_{Di} + \bar{J}_i^2 \sigma_{1i} K_{obs\,i} \right| > \left| 1/2 \bar{J}_i \sigma_{1i} \hat{A}_i(\hat{z}_i, \dot{y}_i) \right| \quad \text{(A19)}$$

for i=1, n where K_{Di} is the i-th element of the diagonal matrix K_D. This results in:

$$\left| K_{Di} + \bar{J}_i^2 \sigma_{1i} K_{obs\,i} \right| > 1/2 \left| \bar{J}_i \right| \sigma_{1i} \hat{A}_i(\hat{z}_i, \dot{y}_i) \quad \text{(A20)}$$

From Eq. 13 it can be observed that $\hat{A}_i(\hat{z}_i, \dot{y}_i)$ increases as the i-th actuator velocity $\dot{y}_i$ increases.

Consider that, given an initial condition, an upper limit to the i-th actuator velocity, $\dot{y}_{i\,max}$, exists. This implies that an upper limit $\hat{A}_{imax} = \hat{A}_i(\hat{z}_i, \dot{y}_{imax})$ exists. Therefore, by choosing $K_{obs\,i}$ according to Eq. A18, and by observing that all terms in the left hand side of Eq. A18 are positive, the gain K_{Di} can be calculated by:

$$K_{Di} > 1/2 \left[\ \left| \bar{J}_i \right| \hat{A}_{imax} - \bar{J}_i^2 K_{obs\,i} \right] \sigma_{1i} \quad \text{(A21)}$$

Under the conditions given by Eq. A18 and Eq. A20, the matrix N_2 is uniformly positive definite, i.e.:

$$N_2 \geq \alpha I \qquad \forall t \geq 0 \quad \text{(A22)}$$

where α is a positive constant given by:

$$\alpha = \inf_{t \in [0,T]} \lambda_{min}(N_2), \quad \forall T \geq 0 \quad \text{(A23)}$$

Using Eq. A22 in Eq. A14 and employing the Rayleight-Ritz theorem results in:

$$\dot{V} \leq -\alpha \left\| \rho \right\|^2 + \left\| \rho \right\| \left\| D(\rho) \right\| \quad \text{(A24)}$$

Since the state vector z is limited (see Dupont et al (2000)), and the elements of the matrix $\tilde{A}(z_{atr}, \hat{z}_{atr}, \dot{y})$ are limited, "disturbance vector" $D(\rho)$ is upper limited, i.e., $\left\| D(\rho) \right\| \leq \bar{D}$. Therefore:

$$\dot{V} \leq -\alpha \left\| \rho \right\|^2 + \bar{D} \left\| \rho \right\| \quad \text{(A25)}$$

The condition in which the time derivative $\dot{V}$ is negative is given by

$$\left\| \rho \right\| > \bar{D} / \alpha \quad \text{(A26)}$$

Expressions A12 and A25 show that $\left\| \rho \right\|$ tends to a residual set, which depends on $\bar{D}$ and on α, as $t \to \infty$. Consequently each error vector component tends to a residual set. So, the measure in the velocity error vector $s_0(t)$ tends to a residual set and, through Eq. 17 we conclude that the tracking errors $\tilde{q}(t)$ and $\dot{\tilde{q}}(t)$ tend to a residual set as $t \to \infty$.

Remark 1: As $\dot{\tilde{q}}(t)$ is limited, the actuator velocity vector $\dot{y}(t)$ is limited. Therefore, there is a velocity upper bound in each actuator, $\dot{y}_{imax}$, which depends on the closed loop system dynamics and of the initial conditions. These initial conditions should satisfy the condition given by Eq. A19. Therefore, the above result depends on the initial conditions. Thus, it is a local result.

Remark 2: The upper bound "disturbance" ($\bar{D}$) depends on the friction characteristics (see Eq. A16) and on the smoothing function $m(\dot{y}_i)$. The positive constant α, defined in Eq. A23 depends on the controller gains. Therefore, the residual set given by Eq. A26 depends on the friction characteristics, on the smoothing and on the controller gains.

Antonio Carlos Valdiero
Was born in Volta Redonda, Brazil, in 1969. He received his Mechanical Engineering degree in 1992, from UFRJ, Brazil, M. Sc. Degree in 1994, from UFSC, Brazil, and Doctoral degree in Mechanical Engineering in 2005, from UFSC, Brazil. Since 1994, he has been a professor at the Technology Department at UNIJUÍ, Brazil.

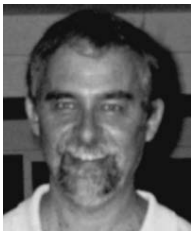

Raul Guenther
Was born in Joinville, Brazil, in 1953. He received his Mechanical Engineering degree, in 1976, from UFSC, Brazil, and D. Sc. in Mechanical Engineering in 1993 from UFRJ, Brazil. Since 1977 he has been a professor at the Department of Mechanical Engineering at UFSC. At the moment, he is the head of the Robotics Laboratory.

Edson Roberto De Pieri
Was born in Mogi Mirim, Brazil, in 1960. He received his Mathematics degree in 1982, and M. Sc. degree in Electrical Engineering in 1987, both from UNICAMP, Brazil. In 1991, he received his D. Sc. degree from the Pierre et Marie Curie University, France. Since 1992 he has been a professor at the Department of Automation and Systems at UFSC.

Victor Juliano De Negri
Was born in São Leopoldo, Brazil. He received his Mechanical Engineering degree in 1983, from UNISINOS, Brazil, M.Eng. degree in 1986, and D.Eng. degree, both from UFSC, Brazil. Since 1995, he has been a professor at the Department of Mechanical Engineering at UFSC. He is currently the head of the Laboratory of Hydraulic and Pneumatic Systems.